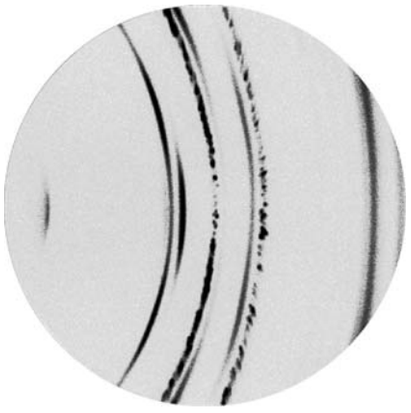

Figure 2.5.2
Diffraction pattern from a battery component containing multiple layers.

1996; Rodriguez-Navarro, 2006). The integrated data give better intensity and statistics for phase ID and quantitative analysis, especially for those samples with texture or large grain sizes, or where the sample is small. Then the integrated diffraction profiles can be analysed with existing algorithms and methods: profile fitting with conventional peak shapes and fundamental parameters, quantification of phases, and lattice-parameter indexing and refinement. The results can be used to search and match to entries in a powder-diffraction database, typically the Powder Diffraction File.

Texture measurement with 2D-XRD is extremely fast compared to measurement using a point or linear detector. The area detector collects texture data and background values simultaneously for multiple poles and multiple directions. Owing to the high measurement speed, pole figures can be measured at very fine steps, allowing detection of very sharp textures (Smith & Ortega, 1993; Bunge & Klein, 1996; He, 2009).

Stress measurement with 2D-XRD is based on a direct relationship between the stress tensor and distortion of the diffraction cones. Since the whole or a part of the diffraction ring is used for stress calculation, 2D-XRD can measure stress with high sensitivity, high speed and high accuracy (He & Smith, 1997; He, 2000). It is highly suitable for samples containing large crystals and textures. Simultaneous measurement of stress and texture is also possible, since 2D data contain both stress and texture information.

Concentrations of crystalline phases can be measured faster and more accurately with data analysis over 2D frames, especially for samples with an anisotropic distribution of crystallite orientations and/or amorphous content. The amorphous region can be defined by the user to consist of regions with no Bragg peaks, or the amorphous region can be defined with the crystalline region included when the crystalline region and the amorphous region overlap.

Microdiffraction data are collected with speed and accuracy. Collection of X-ray diffraction data from small sample amounts or small sample areas has always been a slow process because of limited beam intensity. The 2D detector captures whole or a large portion of the diffraction rings, so spotty, textured or weak diffraction data can be integrated over the selected diffraction rings (Winter & Squires, 1995; Bergese *et al.*, 2001; Tissot, 2003; Bhuvanesh & Reibenspies, 2003; He, 2004). The point beam used for microdiffraction allows diffraction mapping with fine space resolution, even on a curved surface (Allahkarami & Hanan, 2011).

Data can be collected from thin-film samples containing a mixture of single-crystal and polycrystalline layers with random orientation distributions, and highly textured layers, with all the features appearing simultaneously in diffraction frames (Dickerson *et al.*, 2002; He, 2006). The pole figures from different layers and the substrate can be overlapped to reveal the orientation relationships. The use of a 2D detector can dramatically speed up the data collection for reciprocal-space mapping on an in-plane reciprocal-lattice point (Schmidbauer *et al.*, 2008).

Because of the penetrating power of the X-ray beam, fast nondestructive data collection and the abundant information about atomic structure, two-dimensional X-ray diffraction can be used to screen a library of materials with high speed and high accuracy. Two-dimensional X-ray diffraction systems dedicated for combinatorial screening are widely used in the pharmaceutical industry for drug discovery and process analysis (Klein *et al.*, 1998; He *et al.*, 2001).

Forensic science and archaeology have benefited from using two-dimensional X-ray diffraction for identifying materials and structures from small specimens (Kugler, 2003; Bontempi *et al.*, 2008). It is nondestructive and does not require special sample treatment, so the original evidence or sample can be preserved. Two-dimensional diffraction patterns contain abundant information and are easy to observe and explain in the courtroom.

2.5.2. Fundamentals

A conventional powder-diffraction pattern is displayed as the scattering intensity *versus* scattering angle 2θ or d-spacing. A 2D-XRD pattern contains the scattering-intensity distribution as a function of two orthogonal dimensions. One dimension can be expressed in 2θ, which can be interpreted by Bragg's law. The distribution in the dimension orthogonal to 2θ contains additional information, such as the orientation distribution, strain states, and crystallite-size and -shape distribution. In order to understand and analyse 2D diffraction data, new geometry conventions and algorithms are introduced. The geometry conventions and algorithms used for 2D-XRD should also be consistent with conventional XRD, so that many existing concepts and algorithms are still valid when 2D diffraction data are used.

The geometry of a 2D-XRD system can be explained using three distinguishable and interrelated geometry spaces, each defined by a set of parameters (He, 2003). The three geometry spaces are the diffraction space, detector space and sample space. The laboratory coordinate system $\mathbf{X}_L$, $\mathbf{Y}_L$, $\mathbf{Z}_L$ is the basis of all three spaces. Although the three spaces are interrelated, the definitions and corresponding parameters should not be confused. Except for a few parameters introduced specifically for 2D-XRD, many of these parameters are used in conventional X-ray diffraction systems. Therefore, the same definitions are maintained for consistency. The three-circle goniometer in Eulerian geometry is the most commonly used, and all the algorithms for data interpretation and analysis in this chapter are based on Eulerian geometry. The algorithms can be developed for the geometries of other types (such as kappa) by following the same strategies.

2.5.2.1. *Diffraction space and laboratory coordinates*

2.5.2.1.1. *Diffraction cones in laboratory coordinates*

Fig. 2.5.3(*a*) describes the geometric definition of diffraction cones in the laboratory coordinate system $\mathbf{X}_L$, $\mathbf{Y}_L$, $\mathbf{Z}_L$. The laboratory coordinate system is a Cartesian coordinate system.

The plane given by X_L and Y_L is the diffractometer plane. The axis Z_L is perpendicular to the diffractometer plane. The axes X_L, Y_L and Z_L form a right-handed rectangular coordinate system with the origin at the instrument centre. The incident X-ray beam propagates along the X_L axis, which is also the rotation axis of all diffraction cones. The apex angles of the cones are determined by the 2θ values given by the Bragg equation. The apex angles are twice the 2θ values for forward reflection ($2\theta \leq 90^\circ$) and twice the value of $180^\circ - 2\theta$ for backward reflection ($2\theta > 90^\circ$). For clarity, only one diffraction cone of forward reflection is displayed. The γ angle is the azimuthal angle from the origin at the six o'clock direction with a right-handed rotation axis along the opposite direction of incident beam ($-X_L$ direction). A given γ value defines a half plane with the X_L axis as the edge; this will be referred to as the γ plane hereafter. The diffractometer plane consists of two γ planes at $\gamma = 90^\circ$ and $\gamma = 270^\circ$. Therefore many equations developed for 2D-XRD should also apply to conventional XRD if the γ angle is given as a constant of 90° or 270°. A pair of γ and 2θ values represents the direction of a diffracted beam. The γ angle takes a value of 0 to 360° for a complete diffraction ring with a constant 2θ value. The γ and 2θ angles form a spherical coordinate system which covers all the directions from the origin of sample (instrument centre). The γ–2θ system is fixed in the laboratory system $\mathbf{X}_L$, $\mathbf{Y}_L$, $\mathbf{Z}_L$, which is independent of the sample orientation and detector position in the goniometer. 2θ and γ are referred to as the diffraction-space parameters. In the laboratory coordinate system $\mathbf{X}_L$, $\mathbf{Y}_L$, $\mathbf{Z}_L$, the surface of a diffraction cone can be mathematically expressed as

$$y_L^2 + z_L^2 = x_L^2 \tan^2 2\theta, \qquad (2.5.1)$$

with $x_L \geq 0$ or $2\theta \leq 90^\circ$ for forward-diffraction cones and $x_L < 0$ or $2\theta > 90^\circ$ for backward-diffraction cones.

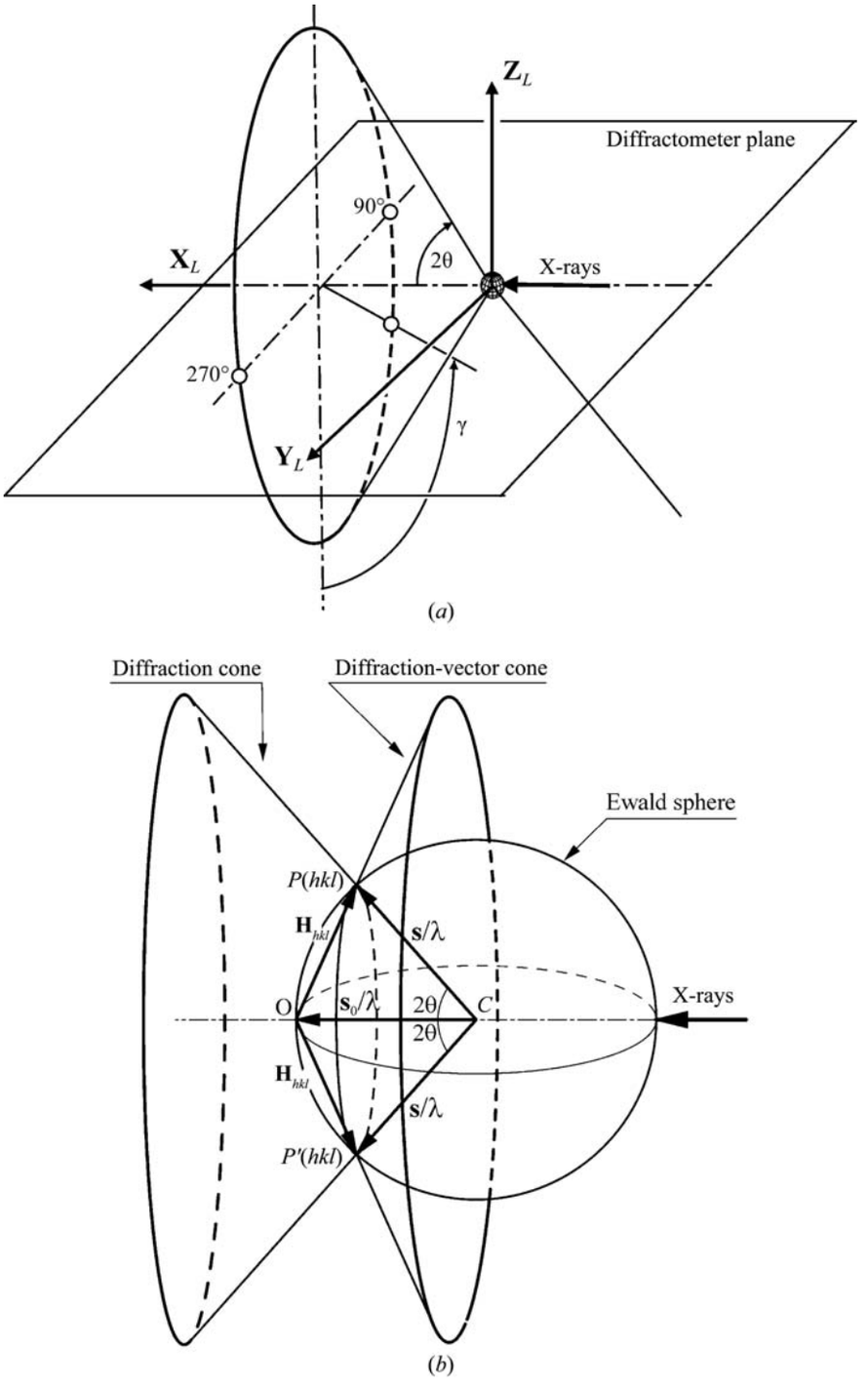

Figure 2.5.3
The diffraction cone and the corresponding diffraction-vector cone.

2.5.2.1.2. *Diffraction-vector cones in laboratory coordinates*

Fig. 2.5.3(*b*) shows the diffraction-vector cone corresponding to the diffraction cone in the laboratory coordinate system. *C* is the centre of the Ewald sphere. The diffraction condition can be given by the Laue equation as

$$\frac{\mathbf{s} - \mathbf{s}_0}{\lambda} = \mathbf{H}_{hkl}, \qquad (2.5.2)$$

where $\mathbf{s}_0$ is the unit vector representing the incident beam, $\mathbf{s}$ is the unit vector representing the diffracted beam and $\mathbf{H}_{hkl}$ is the reciprocal-lattice vector. Its magnitude is given as

$$\left|\frac{\mathbf{s} - \mathbf{s}_0}{\lambda}\right| = \frac{2\sin\theta}{\lambda} = \left|\mathbf{H}_{hkl}\right| = \frac{1}{d_{hkl}}, \qquad (2.5.3)$$

in which d_{hkl} is the d-spacing of the crystal planes (hkl). It can be easily seen that it is the Bragg law in a different form. Therefore, equation (2.5.2) is the Bragg law in vector form. In the Bragg condition, the vectors $\mathbf{s}_0/\lambda$ and $\mathbf{s}/\lambda$ make angles θ with the diffracting planes (hkl) and $\mathbf{H}_{hkl}$ is normal to the (hkl) crystal plane. In order to analyse all the X-rays measured by a 2D detector, we extend the concept to all scattered X-rays from a sample regardless of the Bragg condition. Therefore, the index (hkl) can be removed from the above expression. $\mathbf{H}$ is then a vector which takes the direction bisecting the incident beam and the scattered beam, and has dimensions of inverse length given by $2\sin\theta/\lambda$. Here 2θ is the scattering angle from the incident beam. The vector $\mathbf{H}$ is referred to as the scattering vector or, alternatively, the diffraction vector. When the Bragg condition is

satisfied, the diffraction vector is normal to the diffracting lattice planes and its magnitude is reciprocal to the d-spacing of the lattice planes. In this case, the diffraction vector is equivalent to the reciprocal-lattice vector. Each pixel in a 2D detector measures scattered X-rays in a given direction with respect to the incident beam. We can calculate a diffraction vector for any pixel, even if the pixel is not measuring Bragg scattering. Use of the term 'diffracted beam' hereafter in this chapter does not necessarily imply that it arises from Bragg scattering.

For two-dimensional diffraction, the incident beam can be expressed by the vector $\mathbf{s}_0/\lambda$, but the diffracted beam is no longer in a single direction, but follows the diffraction cone. Since the direction of a diffraction vector is a bisector of the angle between the incident and diffracted beams corresponding to each diffraction cone, the trace of the diffraction vectors forms a cone. This cone is referred to as the diffraction-vector cone. The angle between the diffraction vector and the incident X-ray beam is $90^\circ + \theta$ and the apex angle of a vector cone is $90^\circ - \theta$. It is apparent that diffraction-vector cones can only exists on the $-X_L$ side of the diffraction space.

For two-dimensional diffraction, the diffraction vector is a function of both the γ and 2θ angles, and is given in laboratory coordinates as

$$\mathbf{H} = \frac{\mathbf{s} - \mathbf{s}_0}{\lambda} = \frac{1}{\lambda}\begin{bmatrix} \cos 2\theta - 1 \\ -\sin 2\theta \sin\gamma \\ -\sin 2\theta \cos\gamma \end{bmatrix}. \qquad (2.5.4)$$

The direction of the diffraction vector can be represented by its unit vector, given by

$$\mathbf{h}_L = \frac{\mathbf{H}}{|\mathbf{H}|} = \begin{bmatrix} h_x \\ h_y \\ h_z \end{bmatrix} = \begin{bmatrix} -\sin\theta \\ -\cos\theta \sin\gamma \\ -\cos\theta \cos\gamma \end{bmatrix}, \qquad (2.5.5)$$

where $\mathbf{h}_L$ is a unit vector expressed in laboratory coordinates and the three components in the square brackets are the projections of the unit vector on the three axes of the laboratory coordinates, respectively. If γ takes all values from 0 to 360° at a given Bragg angle 2θ, the trace of the diffraction vector forms a diffraction-vector cone. Since the possible values of θ lie within the range 0 to 90°, h_x takes only negative values.

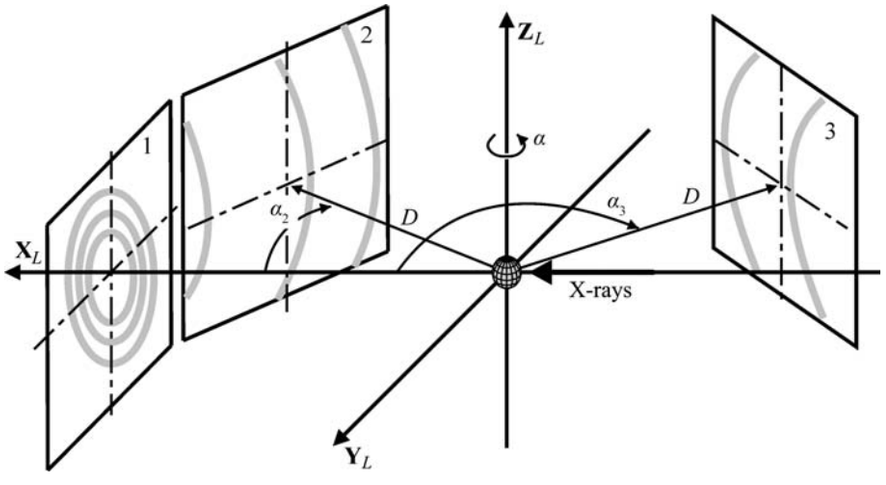

Figure 2.5.4
Detector positions in the laboratory-system coordinates.

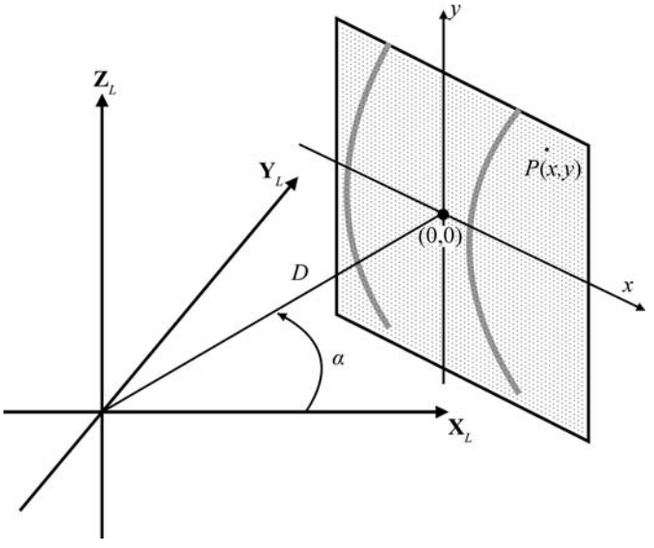

Figure 2.5.5
Relationship between a pixel P and detector position in the laboratory coordinates.

2.5.2.2. *Detector space and pixel position*

A typical 2D detector has a limited detection surface, and the detection surface can be spherical, cylindrical or flat. Spherical or cylindrical detectors are normally designed for a fixed sample-to-detector distance, while a flat detector has the flexibility to be used at different sample-to-detector distances so as to choose either high resolution at a large distance or large angular coverage at a short distance.

2.5.2.2.1. *Detector position in the laboratory system*

The position of a flat detector is defined by the sample-to-detector distance D and the detector swing angle α. D and α are referred to as the detector-space parameters. D is the perpendicular distance from the goniometer centre to the detection plane and α is a right-handed rotation angle about the Z_L axis. Detectors at different positions in the laboratory coordinates X_L, Y_L, Z_L are shown in Fig. 2.5.4. The centre of detector 1 is right on the positive side of the X_L axis (on-axis), $\alpha = 0$. Both detectors 2 and 3 are rotated away from the X_L axis with negative swing angles ($\alpha_2 < 0$ and $\alpha_3 < 0$). The detection surface of a flat 2D detector can be considered as a plane, which intersects the diffraction cone to form a conic section. Depending on the swing angle α and the 2θ angle, the conic section can appear as a circle, an ellipse, a parabola or a hyperbola.

2.5.2.2.2. *Pixel position in diffraction space for a flat detector*

The values of 2θ and γ can be calculated for each pixel in the frame. The calculation is based on the detector-space parameters and the pixel position in the detector. Fig. 2.5.5 shows the relationship of a pixel $P(x, y)$ to the laboratory coordinates X_L, Y_L, Z_L. The position of a pixel in the detector is defined by the (x, y) coordinates, where the detector centre is defined as $x = y = 0$. The diffraction-space coordinates $(2\theta, \gamma)$ for a pixel at $P(x, y)$ are given by

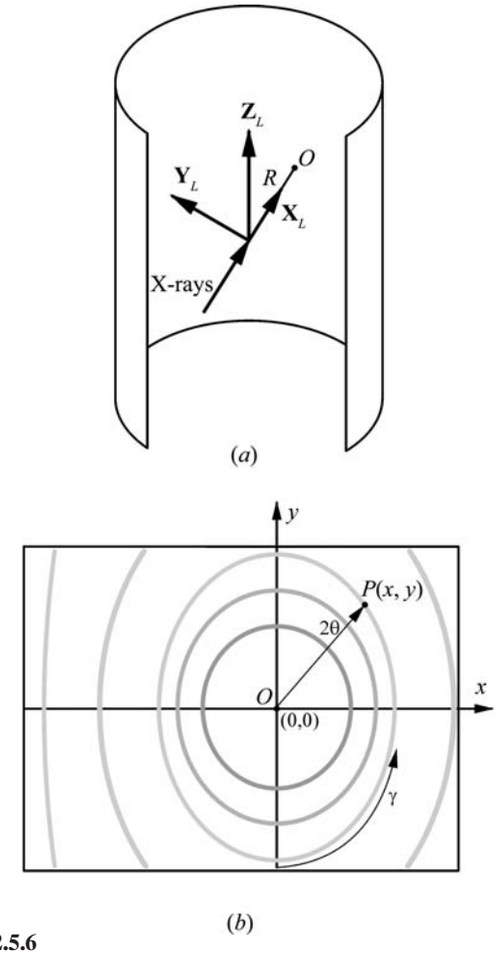

Figure 2.5.6
Cylinder-shaped detector in vertical direction: (*a*) detector position in the laboratory coordinates; (*b*) pixel position in the flattened image.

$$2\theta = \arccos\frac{x\sin\alpha + D\cos\alpha}{(D^2 + x^2 + y^2)^{1/2}} \quad (0 < 2\theta < \pi), \tag{2.5.6}$$

$$\gamma = \frac{x\cos\alpha - D\sin\alpha}{|x\cos\alpha - D\sin\alpha|}\arccos\frac{-y}{[y^2 + (x\cos\alpha - D\sin\alpha)^2)]^{1/2}} \quad (-\pi < \gamma \leq \pi). \tag{2.5.7}$$

2.5.2.2.3. *Pixel position in diffraction space for a curved detector*

The conic sections of the diffraction cones with a curved detector depend on the shape of the detector. The most common curved detectors are cylinder-shaped detectors. The diffraction frame measured by a cylindrical detector can be displayed as a flat frame, typically a rectangle. Fig. 2.5.6(*a*) shows a cylindrical detector in the vertical direction and the corresponding laboratory coordinates X_L, Y_L, Z_L. The sample is located at the origin of the laboratory coordinates inside the cylinder. The incident X-rays strike the detector at a point O if there is no sample or beam stop to block the direct beam. The radius of the cylinder is R. Fig. 2.5.6(*b*) illustrates the 2D diffraction image collected with the cylindrical detector. We take the point O as the origin of the pixel position (0, 0). The diffraction-space coordinates $(2\theta, \gamma)$ for a pixel at $P(x, y)$ are given by

$$2\theta = \arccos\left[R\cos\left(\frac{x}{R}\right)\Big/(R^2 + y^2)^{1/2}\right], \tag{2.5.8}$$

$$\gamma = \frac{x}{|x|}\arccos\left\{-y\Big/\left[y^2 + R^2\sin^2\left(\frac{x}{R}\right)\right]^{1/2}\right\} \quad (-\pi < \gamma \leq \pi). \tag{2.5.9}$$

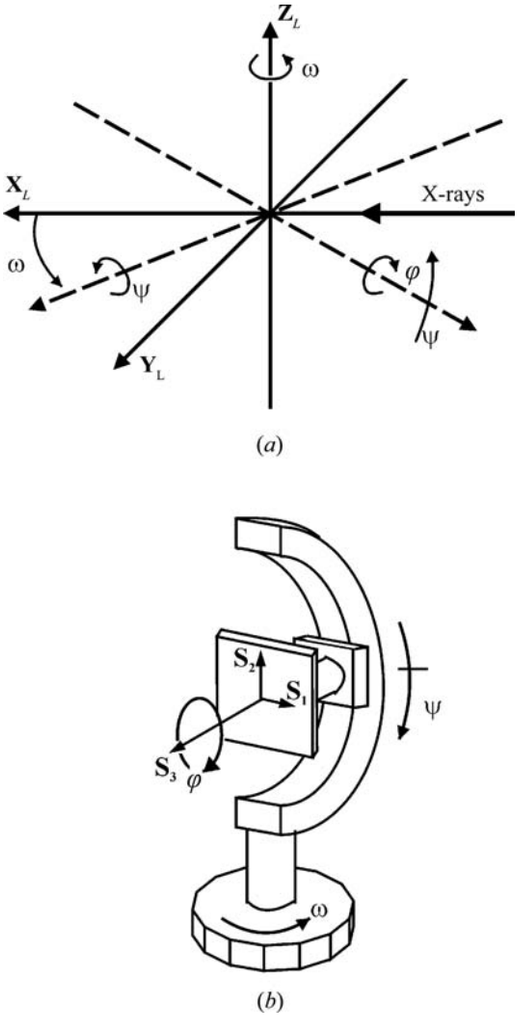

Figure 2.5.7
Sample rotation and translation. (*a*) Three rotation axes in laboratory coordinates; (*b*) rotation axes (ω, ψ, φ) and sample coordinates.

The pixel-position-to-$(2\theta, \gamma)$ conversion for detectors of other shapes can also be derived. Once the diffraction-space coordinates $(2\theta, \gamma)$ of each pixel in the curved 2D detector are determined, most data-analysis algorithms developed for flat detectors are applicable to a curved detector as well.

2.5.2.3. *Sample space and goniometer geometry*

2.5.2.3.1. *Sample rotations and translations in Eulerian geometry*

In a 2D-XRD system, three rotation angles are necessary to define the orientation of a sample in the diffractometer. These three rotation angles can be achieved either by a Eulerian geometry, a kappa (κ) geometry or another kind of geometry. The three angles in Eulerian geometry are ω (omega), ψ (psi) and φ (phi). Fig. 2.5.7(*a*) shows the relationship between rotation axes (ω, ψ, φ) in the laboratory system $\mathbf{X}_L$, $\mathbf{Y}_L$, $\mathbf{Z}_L$. The ω angle is defined as a right-handed rotation about the Z_L axis. The ω axis is fixed in the laboratory coordinates. The ψ angle is a right-handed rotation about a horizontal axis. The angle between the ψ axis and the X_L axis is given by ω. The ψ axis lies on X_L when ω is set at zero. The φ angle defines a left-handed rotation about an axis on the sample, typically the normal of a flat sample. The φ axis lies on the Y_L axis when $\omega = \psi = 0$. In an aligned diffraction system, all three rotation axes and the primary X-ray beam cross at the

origin of the X_L, Y_L, Z_L coordinates. This cross point is also known as the goniometer centre or instrument centre.

Fig. 2.5.7(b) shows the relationship and stacking sequence among all rotation axes (ω, ψ, φ) and the sample coordinates S_1, S_2, S_3. ω is the base rotation; all other rotations and translations are on top of this rotation. The next rotation above ω is the ψ rotation. The next rotation above ω and ψ is the φ rotation. The sample coordinates S_1, S_2, S_3 are fixed to the sample regardless of the particular sample orientation given by the rotation angles (ω, ψ, φ). The φ rotation in the goniometer is intentionally chosen as a left-handed rotation so that the diffraction vectors will make a right-hand rotation observed in the sample coordinates S_1, S_2, S_3.

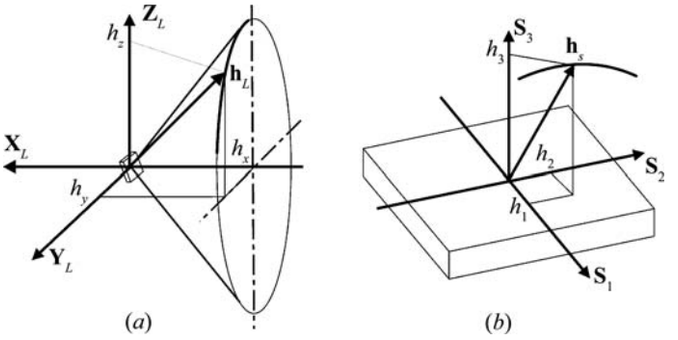

Figure 2.5.8
Unit diffraction vector in (a) the laboratory coordinates and (b) the sample coordinates.

2.5.2.4. *Diffraction-vector transformation*

2.5.2.4.1. *Diffraction unit vector in diffraction space and sample space*

In 2D-XRD data analysis, it is crucial to know the diffraction-vector distribution in terms of the sample coordinates S_1, S_2, S_3. However, the diffraction-vector distribution corresponding to the measured 2D data is always given in terms of the laboratory coordinates X_L, Y_L, Z_L because the diffraction space is fixed to the laboratory coordinates. Fig. 2.5.8 shows the unit vector of a diffraction vector in both (a) the laboratory coordinates X_L, Y_L, Z_L and (b) the sample coordinates S_1, S_2, S_3. In Fig. 2.5.8(a) the unit vector $\mathbf{h}_L$ is projected to the X_L, Y_L and Z_L axes as h_x, h_y and h_z, respectively. The three components are given by equation (2.5.5). In order to analyse the diffraction results relative to the sample orientation, it is necessary to transform the unit vector to the sample coordinates S_1, S_2, S_3. Fig. 2.5.8(b) shows the same unit vector, denoted by $\mathbf{h}_s$ projected to S_1, S_2 and S_3 as h_1, h_2 and h_3, respectively.

2.5.2.4.2. *Transformation from diffraction space to sample space*

The transformation of the unit diffraction vector from the laboratory coordinates X_L, Y_L, Z_L to the sample coordinates S_1, S_2, S_3 is given by

$$\mathbf{h}_s = \boldsymbol{A}\mathbf{h}_L, \tag{2.5.10}$$

where $\boldsymbol{A}$ is the transformation matrix. For Eulerian geometry in matrix form, we have

$$\begin{bmatrix} h_1 \\ h_2 \\ h_3 \end{bmatrix} = \begin{bmatrix} a_{11} & a_{12} & a_{13} \\ a_{21} & a_{22} & a_{23} \\ a_{31} & a_{32} & a_{33} \end{bmatrix} \begin{bmatrix} h_x \\ h_y \\ h_z \end{bmatrix}$$

$$= \begin{bmatrix} -\sin\omega\sin\psi\sin\varphi - \cos\omega\cos\varphi & \cos\omega\sin\psi\sin\varphi - \sin\omega\cos\varphi & -\cos\psi\sin\varphi \\ \sin\omega\sin\psi\cos\varphi - \cos\omega\sin\varphi & -\cos\omega\sin\psi\cos\varphi - \sin\omega\sin\varphi & \cos\psi\cos\varphi \\ -\sin\omega\cos\psi & \cos\omega\cos\psi & \sin\psi \end{bmatrix}$$

$$\times \begin{bmatrix} -\sin\theta \\ -\cos\theta\sin\gamma \\ -\cos\theta\cos\gamma \end{bmatrix}. \tag{2.5.11}$$

In expanded form:

$$\begin{aligned} h_1 &= \sin\theta(\sin\varphi\sin\psi\sin\omega + \cos\varphi\cos\omega) + \cos\theta\cos\gamma\sin\varphi\cos\psi \\ &\quad - \cos\theta\sin\gamma(\sin\varphi\sin\psi\cos\omega - \cos\varphi\sin\omega) \\ h_2 &= -\sin\theta(\cos\varphi\sin\psi\sin\omega - \sin\varphi\cos\omega) \\ &\quad - \cos\theta\cos\gamma\cos\varphi\cos\psi \\ &\quad + \cos\theta\sin\gamma(\cos\varphi\sin\psi\cos\omega + \sin\varphi\sin\omega) \\ h_3 &= \sin\theta\cos\psi\sin\omega - \cos\theta\sin\gamma\cos\psi\cos\omega - \cos\theta\cos\gamma\sin\psi \end{aligned} \tag{2.5.12}$$

In addition to the diffraction intensity and Bragg angle corresponding to each data point on the diffraction ring, the unit vector $\mathbf{h}_s\{h_1, h_2, h_3\}$ provides orientation information in the sample space. The transformation matrix of any other goniometer geometry, such as kappa geometry (Paciorek *et al.*, 1999), can be introduced into equation (2.5.10) so that the unit vector $\mathbf{h}_s\{h_1, h_2, h_3\}$ can be expressed in terms of the specified geometry. All equations using the unit vector $\mathbf{h}_s\{h_1, h_2, h_3\}$ in this chapter, such as in data treatment, texture analysis and stress measurement, are applicable to all goniometer geometries provided that the unit-vector components are generated from the corresponding transformation matrix from diffraction space to the sample space.

2.5.2.4.3. *Transformation from detector space to reciprocal space*

Reciprocal-space mapping is commonly used to analyse the diffraction patterns from highly oriented structures, diffuse scattering from crystal defects, and thin films (Hanna & Windle, 1995; Mudie *et al.*, 2004; Smilgies & Blasini, 2007; Schmidbauer *et al.*, 2008). The equations of the unit-vector calculation given above can also be used to transform the diffraction intensity from the diffraction space to the reciprocal space with respect to the sample coordinates. The direction of the scattering vector is given by the unit vector $\mathbf{h}_s\{h_1, h_2, h_3\}$ and the magnitude of the scattering vector is given by $2\sin\theta/\lambda$, so that the scattering vector corresponding to a pixel is given by

$$\mathbf{H} = \frac{2\sin\theta}{\lambda}\mathbf{h}_s. \tag{2.5.13}$$

The three-dimensional reciprocal-space mapping can be obtained by applying the normalized pixel intensities to the corresponding reciprocal points. With various sample orientations, all pixels on the detector can be mapped into a 3D reciprocal space.

references